Approximate normal mode analysis based on vibrational subsystem analysis with high accuracy and efficiency

Jeffrey Hafner and Wenjun Zheng[a)]
Department of Physics, University at Buffalo, Buffalo, New York 14260, USA

(Received 17 March 2009; accepted 3 May 2009; published online 20 May 2009)

Normal mode analysis (NMA) has been proven valuable in modeling slow conformational dynamics of biomolecular structures beyond the reach of direct molecular simulations. However, it remains computationally expensive to directly solve normal modes for large biomolecular systems. In this study, we have evaluated the accuracy and efficiency of two approximate NMA protocols—one based on our recently proposed vibrational subsystem analysis (VSA), the other based on the rotation translation block (RTB), in comparison with standard NMA that directly solves a full Hessian matrix. By properly accounting for flexibility within blocks of residues or atoms based on a subsystem-environment partition, VSA-based NMA has attained a much higher accuracy than RTB and much lower computing cost than standard NMA. Therefore, VSA enables accurate and efficient calculations of normal modes from all-atom or coarse-grained potential functions, which promise to improve conformational sampling driven by low-frequency normal modes. © *2009 American Institute of Physics*. [DOI: 10.1063/1.3141022]

I. INTRODUCTION

Conformational dynamics plays key roles in the functions of various biomolecular systems from enzymes to motor proteins.[1,2] Of particular interests is the "slow" dynamics (microseconds to minutes) in large biomolecular complexes, which is far beyond the simulation time scales (tens of nanoseconds) of atomistic molecular dynamics (MD) (Ref. 3) using modern computers.[4] To capture such slow dynamics, normal mode analysis (NMA)[5–8] has been widely utilized, which solves the eigenmodes of the Hessian matrix calculated from either all-atom or coarse-grained potential functions. Although the all-atom NMA is computationally less expensive than long-time MD simulations, the $O(N^3)$ computing time and the $O(N^2)$ memory requirement (N is the number of atoms in the system) have hindered its application to large systems.

By reducing the number of degrees of freedom ($3N$), the coarse-grained (low resolution) modeling[9] has greatly extended the applicability of NMA to large biomolecular systems. A prime example of coarse-grained models is the elastic network model (ENM) which represents a protein structure as a network of C_α atoms locally connected by springs.[10–12] In an ENM, the all-atom force fields are replaced by simple harmonic potentials with a uniform force constant.[13] Early studies have shown that the large-scale collective motions predicted by the NMA of ENM are insensitive to the dramatic simplification in ENM.[10–12] The low-frequency modes calculated from ENM were found to compare well with many large-scale domain motions observed crystallographically.[12,14] Numerous studies have established the ENM as an efficient means to probe the functionally relevant conformational dynamics from biomolecular structures with virtually no limit in time scale or system size.[15–17] Indeed, ENM has been applied to large biomolecular complexes such as ribosome,[18,19] chaperonin GroEL,[20,21] and viral capsids.[22,23] Further coarse graining is needed to tackle even larger biomolecular or cellular systems.

The growing need for applying NMA to large biomolecular structures has motivated the development of approximate NMA methods to solve the low-frequency modes with less CPU time than standard NMA of the full Hessian matrix. To this end, NMA techniques based on rotations and translations of rigid blocks (RTB)[24–26] have been advanced. These methods assume that low-frequency normal modes of protein structures can be approximated as rigid-body motions of "blocks" with six degrees of freedom per block. Here a block is often defined as a group of sequentially consecutive residues. Therefore, the total number of degrees of freedom is greatly reduced from $3N$ to $6N_b$ (N is the number of atoms and N_b is the number of blocks). RTB was shown to reproduce the lowest-frequency modes with reasonable accuracy and very low computing cost.[24–26]

The assumption of rigidity in RTB ignores the local flexibility within individual blocks. So RTB cannot fully account for local changes in structure and energy. Although such local inaccuracy does not significantly affect the ability of low-frequency modes to capture the global features of collective protein motions, it may become serious when the approximate normal modes are used to guide the conformational sampling, where local structural flexibility is important. Therefore, an approximate NMA technique that incorporates local flexibility is needed to complement RTB in treating both local and global structural changes properly.

In a recent study, one of us has proposed the subsystem NMA based on ENM (Ref. 27) which calculates the "local modes" for a subset of a protein structure (named subsystem)

[a)]Electronic mail: wjzheng@buffalo.edu.

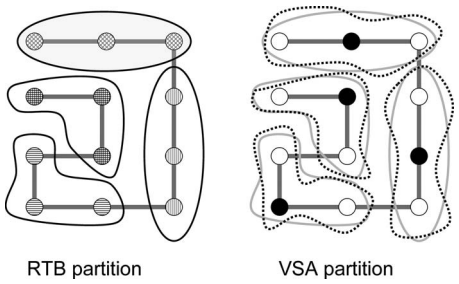

FIG. 1. A cartoon example for partitioning a protein structure into rigid blocks (in RTB) and flexible blocks (in VSA): protein residues are represented by spheres, which are sequentially connected by peptide bonds (shown as thick lines). Four blocks are shown. Each block corresponds to a segment of three consecutive residues along the protein sequence. In total, there are 24 RTB modes and 12 VSA modes. In VSA partition, subsystem (environment) residues are represented by black (white) spheres.

while treating the rest as fast-fluctuating "environment." This method has been employed to analyze the active-site dynamics of two motor proteins (myosin and kinesin)[27] and ATP-binding induced conformational changes in NS3 helicase.[28] It was recently reformulated as the vibrational subsystem analysis (VSA) method for coupling global motions to a local subsystem with all-atom representations and hybrid quantum mechanical/molecular mechanical potentials.[29]

One promising application of VSA is to perform approximate NMA—an all-atom or C_α-only protein structure is first partitioned into a set of blocks, then one representative C_α atom per block is selected to make up the subsystem while the rest is treated as environment, then the normal modes (named VSA modes) are solved for the effective Hessian matrix of the subsystem (see Sec. II). For the structural motions described by VSA modes, the environment residues can fully fluctuate by following the movements of "subsystem" residues. Therefore, VSA allows us to account for flexibility within blocks which is ignored in RTB-based NMA. This advantage is achieved with fewer normal modes than RTB (the total number of modes is $3N_b$ for VSA and $6N_b$ for RTB, where N_b is the number of blocks). For a cartoon example that demonstrates the differences between RTB and VSA, see Fig. 1.

Although VSA has been well established by previous studies,[27–29] its efficiency and accuracy have not been fully tested in comparison with alternative NMA methods (such as RTB), especially for large biomolecular systems. Compared with standard NMA, VSA requires the additional calculation of the effective Hessian matrix for subsystem which involves the inversion of the Hessian submatrix of the environment (see Sec. II). To enable practical applications of VSA to large biomolecular systems, it is important to implement VSA efficiently to minimize this computing overhead. The accuracy and efficiency of the VSA-based NMA must be assessed in comparison with alternative state-of-the-art NMA methods.

In this study, we have implemented the VSA-based NMA using a highly efficient sparse linear-equation solver named CHOLMOD.[30] Then we have evaluated its performance in solving low-frequency normal modes for Hessian matrices based on either coarse-grained ENM or all-atom potential function. Three large protein structures (F_1 ATPase with ~3000 residues, chaperonin GroEL-GroES with >8000 residues, and myosin II motor domain with >10 000 atoms) are used for the evaluation. The efficiency and accuracy of VSA-based NMA are compared with the standard NMA that solves full Hessian matrices using a sparse eigensolver named BLZPACK (Ref. 24) and the RTB-based NMA.[24] The VSA-based NMA is found to be significantly faster than BLZPACK (up to >10 times) but slower than RTB, while its accuracy is much higher than RTB. Therefore, VSA makes a unique addition to the spectrum of NMA methods with balanced efficiency and accuracy.

II. METHODS

A. Formulation of VSA

Here we seek approximate solution of the normal modes for the Hessian matrix of a two-component (S: subsystem, E: environment) harmonic system

$$\begin{bmatrix} H_{SS} & H_{SE} \\ H_{ES} & H_{EE} \end{bmatrix} \begin{bmatrix} V_S \\ V_E \end{bmatrix} = \lambda \begin{bmatrix} M_S & 0 \\ 0 & M_E \end{bmatrix} \begin{bmatrix} V_S \\ V_E \end{bmatrix}, \tag{1}$$

where M_S (M_E) represents the diagonal mass submatrix of S (E) component, V_S (V_E) denotes the S (E) component of an eigenvector, and λ is the corresponding eigenvalue.

Then we rewrite Eq. (1) as

$$\begin{aligned} H_{SE}V_E &= (\lambda M_S - H_{SS})V_S, \\ H_{ES}V_S &= (\lambda M_E - H_{EE})V_E. \end{aligned} \tag{2}$$

After removing the V_E variable, we obtain the following nonlinear eigenequation for V_S:

$$H_{SE}(\lambda M_E - H_{EE})^{-1}H_{ES}V_S = (\lambda M_S - H_{SS})V_S. \tag{3}$$

At the limit of small λ,

$$(\lambda M_E - H_{EE})^{-1} \approx -H_{EE}^{-1} - \lambda H_{EE}^{-1}M_E H_{EE}^{-1}. \tag{4}$$

So Eq. (3) can be approximately reduced to a linear eigenequation as follows:

$$H_{SS}^{\text{eff}}V_S = \lambda M_S^{\text{eff}}V_S, \tag{5}$$

where

$$\begin{aligned} H_{SS}^{\text{eff}} &= H_{SS} - H_{SE}H_{EE}^{-1}H_{ES}, \\ M_S^{\text{eff}} &= M_S + H_{SE}H_{EE}^{-1}M_E H_{EE}^{-1}H_{ES}. \end{aligned} \tag{6}$$

Thus the solution of eigenmodes for a full Hessian matrix [Eq. (1)] is reduced to a generalized eigenproblem with smaller dimension (Eq. (5)).

After solving V_S from Eq. (5), the corresponding V_E is solved as follows:

$$\begin{aligned} V_E &= (\lambda M_E - H_{EE})^{-1}H_{ES}V_S \\ &\approx -H_{EE}^{-1}H_{ES}V_S - \lambda H_{EE}^{-1}M_E H_{EE}^{-1}H_{ES}V_S. \end{aligned} \tag{7}$$

B. Implementation of VSA and RTB

Under the condition of $N_S \ll N_E$ (N_S: number of residues/atoms in subsystem, N_E: number of residues/atoms in environment), the NMA of a full Hessian matrix is reduced to the

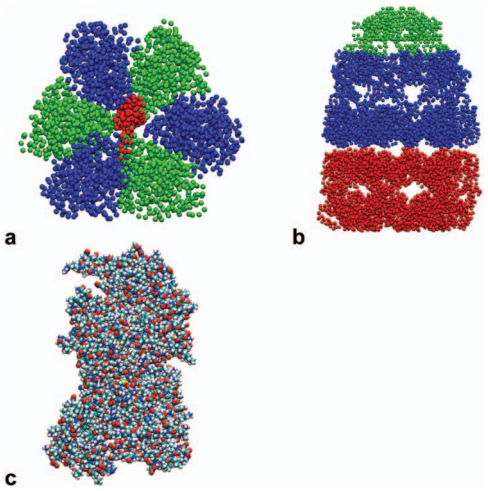

FIG. 2. (Color) Three test cases of large protein structures: (a) F_1 ATPase (PDB: 1BMF); (b) Chaperonin GroEL-GroES (PDB: 1AON); (c) An all-atom model of myosin II motor domain (built from PDB: 1VOM).

NMA of a significantly smaller effective Hessian matrix H_{SS}^{eff}. The computing overhead for the calculation of H_{SS}^{eff} involves the solution of linear equations $H_{EE}^{-1}H_{ES}$ (the inversion of H_{EE} assumes the absence of zero modes for H_{EE}, which is generally true). These calculations can be done efficiently using the Cholesky factorization technique for sparse and positive definitive matrices [as implemented in CHOLMOD (Ref. 30)]. The NMA of H_{SS}^{eff} is performed using the generalized eigensolver subroutine DSYGVX from LAPACK (http://www.netlib.org/lapack/).

For comparison, RTB-based NMA was implemented by using BLZPACK to solve normal modes for the following reduced RTB Hessian matrix:[24]

$$H_{\text{RTB}} = P^T H P, \tag{8}$$

where P is an orthogonal matrix built with vectors associated with the rotations and translations of each block[24] and H is the full Hessian matrix.

C. Test cases

We have assessed the accuracy and efficiency of VSA-based NMA compared with RTB-based NMA and full Hessian eigensolver BLZPACK using three large protein structures (see Fig. 2). Two crystal structures of F_1 ATPase (PDB: 1BMF with 2987 residues) and chaperonin GroEL-GroES (PDB: 1AON with 8015 residues) are used to construct C_α-based ENM with a cutoff distance of 10 Å and two force constants ($C_1=1$ between nonbonded residues and $C_2=100$ between bonded residues). Then a Hessian matrix is computed from the ENM potential function[13] and solved by the above three NMA protocols. The entire structure is divided into blocks of 3–20 residues for RTB-based and VSA-based NMA (each block corresponds to a segment of consecutive residues along the protein sequence, see Fig. 1).

Starting from a myosin II crystal structure (PDB: 1VOM), an all-atom structural model (with 11970 atoms) was built by using MODLOOP (Ref. 31) to add disordered loops and HBUILD to add hydrogen atoms.[32] The nonprotein ligands are deleted for simplicity. Then CHARMM program[33] is used to perform energy minimization with CHARMM22 force field (nonbonded parameters: ATOM FSHIFT CDIE VDW VSHIFT CUTNB 13.0 CTOFNB 12.0 CTONNB 8.0 WMIN 1.5 EPS 1.0). Then the VIBRAN module of CHARMM is used to calculate the all-atom Hessian matrix, which is then solved by the above three NMA protocols. The entire structure is divided into blocks of 1–10 residues for RTB-based and VSA-based NMA.

D. Evaluation of accuracy and efficiency of VSA and RTB

To evaluate the accuracy of low-frequency normal modes solved by VSA-based and RTB-based NMA, we have compared the eigenvalues and eigenvectors of the VSA/RTB modes with those of the exact modes solved from the full Hessian matrix by BLZPACK.

We compute the overlaps (absolute value of dot product) between the eigenvector of the lowest ten VSA/RTB modes (named as mode m_a) and the lowest 15 exact modes and find the exact mode with the maximal overlap (named as mode m_e). Then the overlap between mode m_a and mode m_e gives the accuracy of the eigenvector of mode m_a (an overlap close to 1 indicates high accuracy). The ratio between the eigenvalue of mode m_e and mode m_a gives the accuracy of the eigenvalue of mode m_a (a ratio close to 1 indicates high accuracy). Finally the maximal overlaps and eigenvalue ratios are averaged over the lowest ten VSA/RTB modes to quantify their average accuracy.

To assess the computing cost, the three NMA protocols are run on a dual quad core Xeon work station (2.5 GHZ) with 32GB memory, and the CPU times (clock time) are compared.

III. RESULTS AND DISCUSSION

We have assessed the accuracy and efficiency of VSA-based NMA in comparison with RTB-based NMA and a full Hessian eigensolver BLZPACK using three test cases (see Sec. II). The full Hessian matrices are calculated from a coarse-grained ENM potential (cases 1 and 2) or an all-atom empirical force field (case 3). The chosen protein systems are much larger than the ones studied previously by VSA.[27–29]

A. Evaluation of accuracy

To evaluate the accuracy of the VSA-based and RTB-based NMA, we have compared the eigenvalues and eigenvectors of the lowest ten VSA/RTB modes with those of the exact modes solved by BLZPACK (see Sec. II). The eigenvector accuracy is assessed by the maximal overlap between a VSA/RTB mode and exact modes. The eigenvalue accuracy is assessed by the ratio of eigenvalue between a VSA/RTB mode and the corresponding exact mode (see Sec. II). The results of three test cases are discussed as follows.

Case 1: F_1 ATPase [Fig. 2(a)]

The accuracy of both VSA and RTB declines as block size increases from 3 to 20 despite some fluctuations [see Fig. 3(b)]. The accuracy of VSA decreases slower than RTB as block size increases [see Fig. 3(b)]. For a block size of 20,

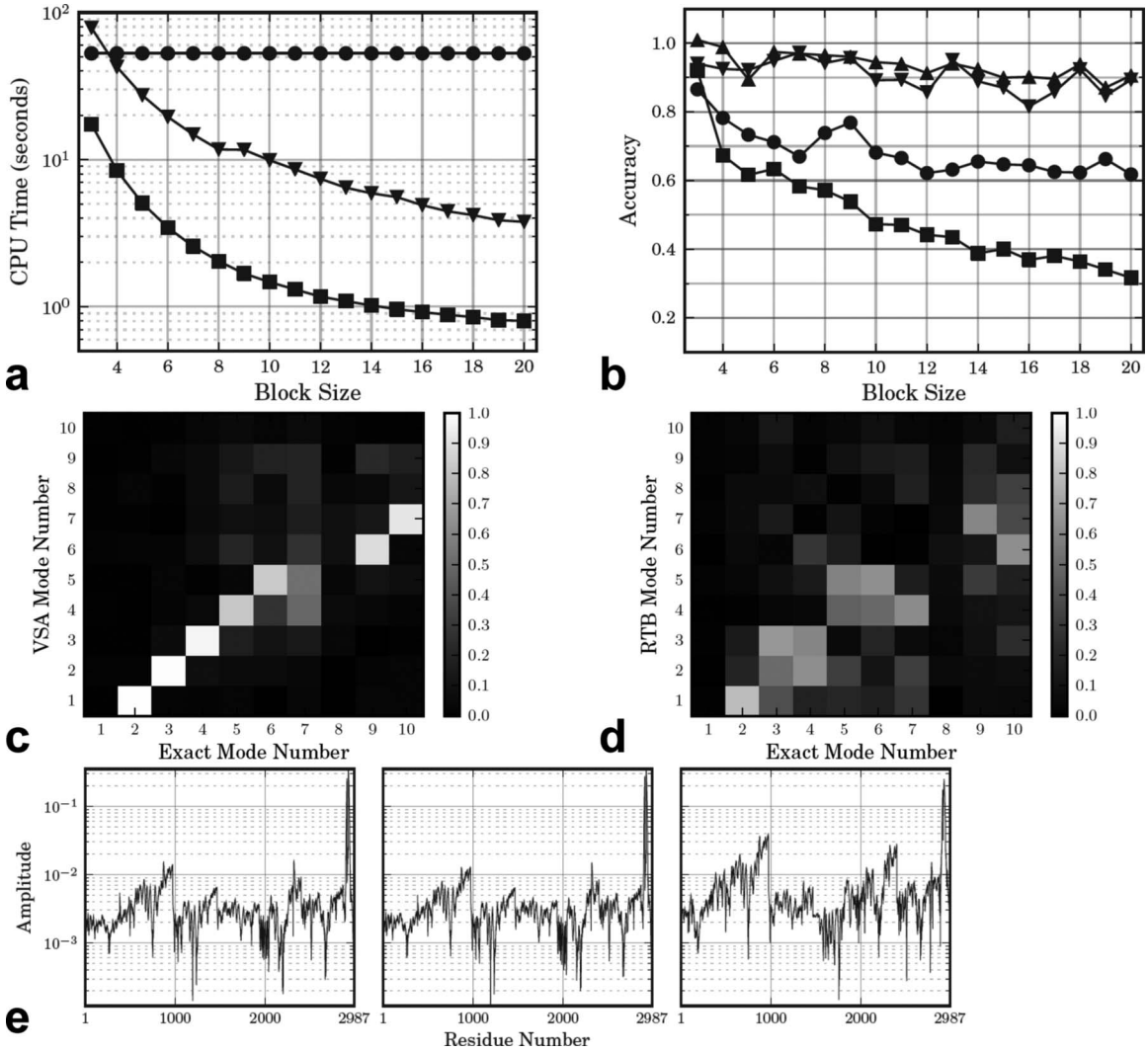

FIG. 3. Evaluation of accuracy and computing cost of VSA-based, RTB-based, and exact NMA for Case 1 (PDB: 1BMF): (a) CPU time of exact (●), VSA-based (▼), RTB-based (■) NMA as a function of block size (in logarithmic scale); (b) Average accuracy of the lowest ten VSA/RTB modes as a function of block size: VSA eigenvalues (▲), VSA eigenvectors (▼), RTB eigenvalues (■), RTB eigenvectors (●); (c) Pairwise comparison in eigenvector between the lowest ten VSA modes (block size=20) and exact modes; (d) Pairwise comparison in eigenvector between the lowest ten RTB modes (block size=20) and exact modes; (e) Eigenvector amplitude as a function of residue position for the VSA mode 1 (left panel), exact mode 2 (middle panel), and the RTB mode 1 (right panel).

the lowest ten VSA eigenvectors have an average overlap of ~0.89 with the corresponding exact modes, while the lowest ten RTB eigenvectors have an average overlap of ~0.62. The VSA eigenvalues also compare much better with exact modes (with average ratio of ~0.91) than RTB eigenvalues (with average ratio of ~0.32).

For a block size of 20, an all-to-all pairwise comparison in eigenvector between the lowest ten VSA/RTB modes and the lowest ten exact modes is shown in Figs. 3(c) and 3(d). The VSA modes 1–7 compare well (with overlap >0.8) with the exact modes 2–6, 9, and 10, respectively, while only the RTB mode 1 compares well (with overlap >0.8) with the exact mode 2. For VSA mode 1, the eigenvector amplitude as a function of residue position nearly coincides with that of the exact mode 2 [see Fig. 3(e)], while significant differences exist between the RTB mode 1 and the exact mode 2 [see Fig. 3(e)]. Both methods fail to capture the exact modes 1 and 8 because they involve highly localized motions within a block. Overall, VSA offers a significantly more accurate approximation to the lowest ten exact modes than RTB.

Case 2: Chaperonin GroEL-GroES [Fig. 2(b)]

The improvement in accuracy from RTB to VSA is even more substantial in this case [see Fig. 4(b)]. For a block size of 20, the lowest ten VSA eigenvectors have an average overlap of ~1.00 with the corresponding exact modes, while the lowest ten RTB eigenvectors have an average overlap of ~0.68. The VSA eigenvalues also compare much better with the exact modes (with average ratio of ~0.98) than RTB eigenvalues (with average ratio of ~0.31).

For a block size of 20, an all-to-all pairwise comparison in eigenvector between the lowest ten VSA/RTB modes and the lowest ten exact modes is shown in Figs. 4(c) and 4(d). The VSA modes 1–10 are nearly identical (with overlap of ~1.0) to the exact modes 1–10, while only RTB modes 1–3 compare well (with overlap >0.8) with the exact modes 1–3. For VSA mode 1, the eigenvector amplitude as a function of residue position essentially coincides with that of the exact mode 1 [see Fig. 4(e)], while significant differences exist between the RTB mode 1 and the exact mode 1 [see Fig. 4(e)].

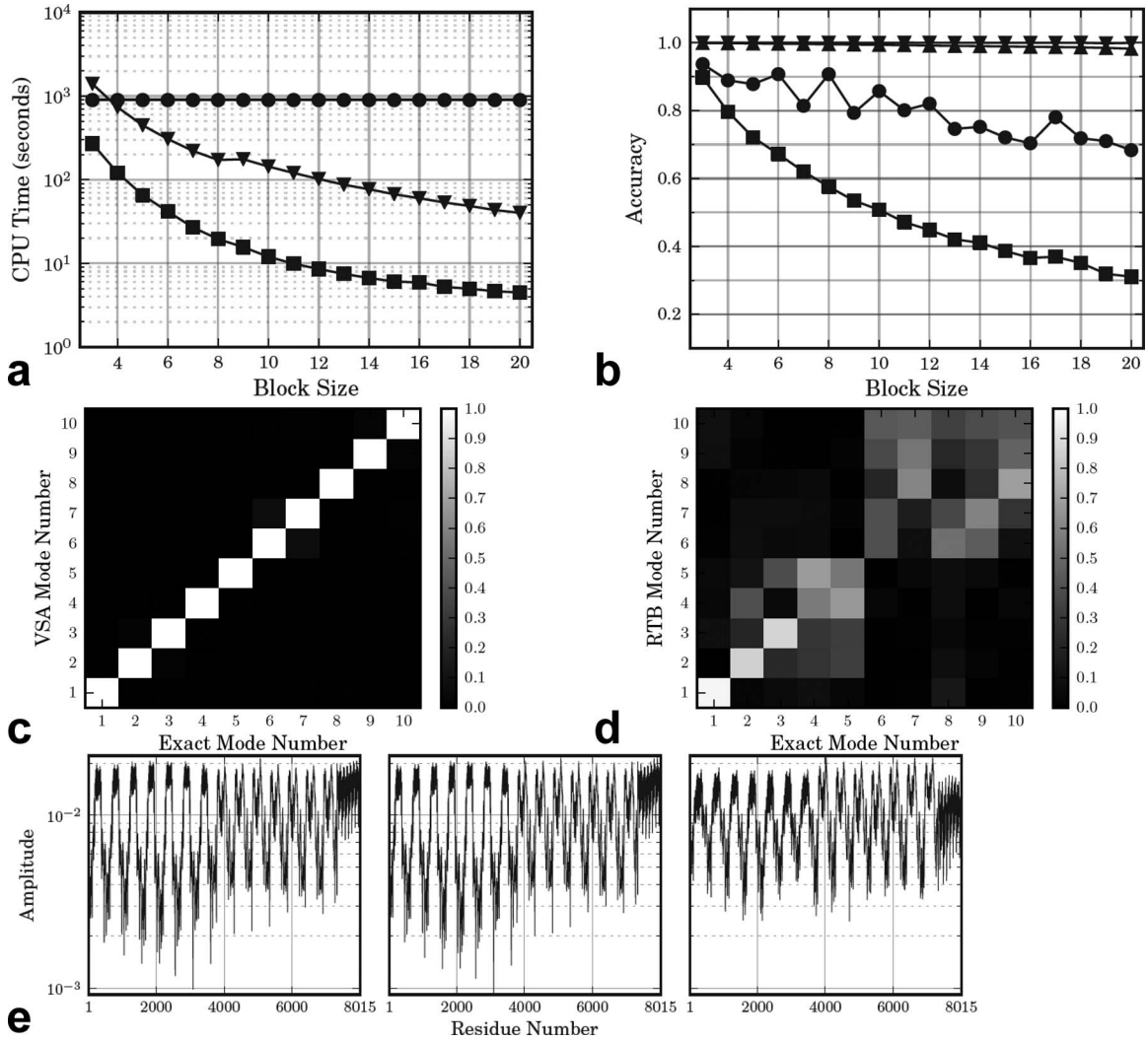

FIG. 4. Evaluation of accuracy and computing cost of VSA-based, RTB-based, and exact NMA for Case 2 (PDB: 1AON): (a) CPU time of exact (●), VSA-based (▼), RTB-based (■) NMA as a function of block size (in logarithmic scale); (b) Average accuracy of the lowest ten VSA/RTB modes as a function of block size: VSA eigenvalues (▲), VSA eigenvectors (▼), RTB eigenvalues (■), RTB eigenvectors (●); (c) Pairwise comparison in eigenvector between the lowest ten VSA modes (block size=20) and exact modes; (d) Pairwise comparison in eigenvector between the lowest ten RTB modes (block size=20) and exact modes; (e) Eigenvector amplitude as a function of residue position for the VSA mode 1 (left panel), exact mode 1 (middle panel), and the RTB mode 1 (right panel).

Case 3: Myosin II motor domain [Fig. 2(c)]

In this case, we calculate the normal modes for the all-atom Hessian matrix computed from the CHARMM22 force field (see Sec. II). The improvement in accuracy from RTB to VSA is substantial [see Fig. 5(b)]. For a block size of ten residues, the lowest ten VSA eigenvectors have an average overlap of ~0.88 with the corresponding exact modes, while the lowest ten RTB eigenvectors have an average overlap of ~0.60. The VSA eigenvalues also compare much better with the exact modes (with average ratio of ~0.93) than RTB eigenvalues (with average ratio of ~0.07).

For a block size of ten, an all-to-all pairwise comparison in eigenvector between the lowest ten VSA/RTB modes and the lowest ten exact modes is shown in Figs. 5(c) and 5(d). The VSA modes 1–5, 8, and 10 compare well (with overlap >0.8) with the exact modes 1–5, 9, and 10, respectively, while only the RTB mode 1 compares well (with overlap >0.8) with the exact mode 1. For the VSA mode 1, the eigenvector amplitude as a function of atom position nearly coincides with that of the exact mode 1 [see Fig. 5(e)], while visible differences exist between the RTB mode 1 and the exact mode 1 [see Fig. 5(e)].

In summary, the accuracy of VSA-based NMA is significantly higher than RTB-based NMA especially for a large block size. The improvement in accuracy is particularly high for eigenvalues, which RTB significantly underestimates for the lack of local flexibility within the blocks.

B. Evaluation of efficiency

To establish the practical value of an approximate method such as VSA, both accuracy and efficiency relative to the exact method must be demonstrated. Compared with the exact NMA of full Hessian matrix, VSA only solves an effective Hessian matrix H_{SS}^{eff} with a reduced dimension (see Sec. II). However, VSA has a computing overhead for the calculation of H_{SS}^{eff}, which involves the solution of linear equations $H_{EE}^{-1}H_{ES}$. A tradeoff between these two opposing

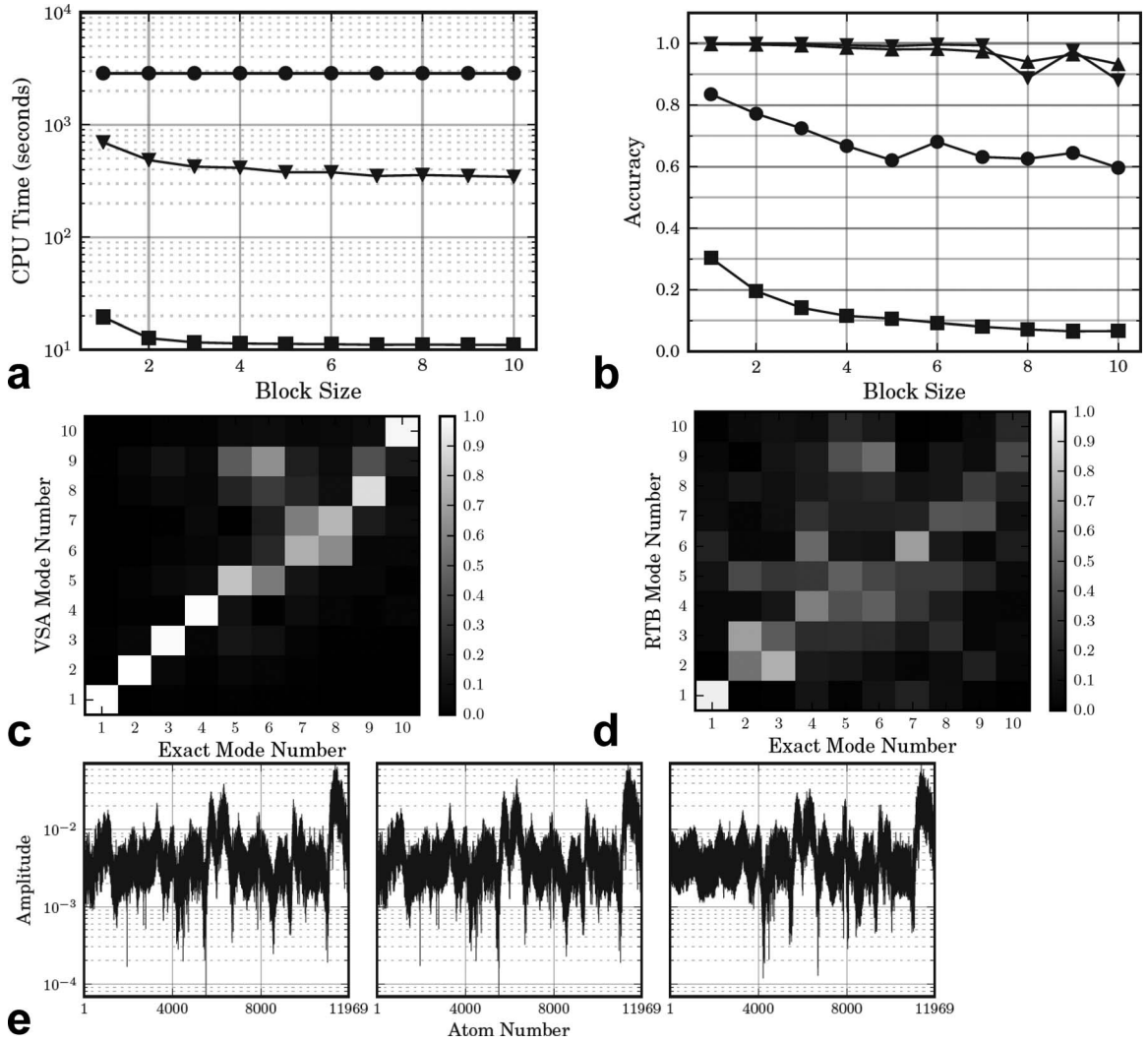

FIG. 5. Evaluation of accuracy and computing cost of VSA-based, RTB-based, and exact NMA for Case 3 (myosin II all-atom model): (a) CPU time of exact (●), VSA-based (▼), RTB-based (■) NMA as a function of block size (in logarithmic scale); (b) Average accuracy of the lowest ten VSA/RTB modes as a function of block size: VSA eigenvalues (▲), VSA eigenvectors (▼), RTB eigenvalues (■), RTB eigenvectors (●); (c) Pairwise comparison in eigenvector between the lowest ten VSA modes (block size=10) and exact modes; (d) Pairwise comparison in eigenvector between the lowest ten RTB modes (block size=10) and exact modes; (e) Eigenvector amplitude as a function of atom position for the VSA mode 1 (left panel), exact mode 1 (middle panel), and the RTB mode 1 (right panel).

factors determines the computing cost of VSA. To calibrate the efficiency of VSA, we compare the CPU times for solving the lowest ten normal modes using the VSA-based NMA, RTB-based NMA, and exact NMA using BLZPACK, respectively. The results for three test cases are discussed as follows.

Case 1: F_1 ATPase [Fig. 3(a)]

The computing cost of VSA (CPU time ~ 79 s) is comparable to the exact NMA (CPU time ~ 53 s) for block size of three. As the block size increases from 3 to 20, the CPU time of VSA decreases significantly (from 79 to 4 s). For a block size of 20, VSA is ~14 times faster than the exact NMA. For a larger block size the CPU time of VSA becomes flat. For a block size between 3 and 20, RTB is about 4.5 times faster than VSA.

Case 2: Chaperonin GroEL-GroES [Fig. 4(a)]

Similar to Case 1, as block size increases from 3 to 20, the CPU time of VSA decreases significantly (from 1399 to 40 s). For a block size of 20, VSA is ~22 times faster than the exact NMA. For a block size between 3 and 20, RTB is 5–9 times faster than VSA.

Case 3: Myosin II motor domain [Fig. 5(a)]

The computing cost of VSA (CPU time ~ 698 s) is ~7 times lower than the exact NMA (CPU time ~ 2880 s) for a block size of one residue. As block size increases from one to ten, the CPU time of VSA decreases by ~50% (from 698 to 344 s). For a block size between one and ten, RTB is >30 times faster than VSA.

In summary, the efficiency of VSA is intermediate between exact NMA and RTB. VSA is much faster than the exact NMA especially for a large block size. RTB is even faster than VSA.

IV. CONCLUSION

We have evaluated the accuracy and efficiency of two approximate NMA protocols (VSA based and RTB based) in

comparison with standard NMA that directly solves a full Hessian matrix. By properly accounting for flexibility within the blocks based on subsystem-environment partition,[27] VSA-based NMA has attained a much higher accuracy than RTB and much lower computing cost than standard NMA. Therefore, VSA enables accurate and efficient calculations of normal modes from all-atom or coarse-grained potential functions, which promise to improve conformational sampling driven by low-frequency normal modes.

Our evaluation suggests that RTB remains a most efficient option for solving low-frequency normal modes of large biomolecular systems especially if high accuracy in eigenvalue or eigenvector is not required.

In the future, we will combine VSA-based NMA with our previously developed methods for coarse-grained modeling of the conformational fluctuations[34] and transitions[35] in large biomolecular systems.

ACKNOWLEDGMENTS

This study is supported by the funding from University at Buffalo and a grant from AHA (Grant No. 0835292N).

[1] K. Henzler-Wildman and D. Kern, Nature (London) **450**, 964 (2007).
[2] M. Gerstein and N. Echols, Curr. Opin. Chem. Biol. **8**, 14 (2004).
[3] M. Karplus and J. A. McCammon, Nat. Struct. Biol. **9**, 646 (2002).
[4] R. Elber, Curr. Opin. Struct. Biol. **15**, 151 (2005).
[5] B. R. Brooks, D. Janezic, and M. Karplus, J. Comput. Chem. **16**, 1522 (1995).
[6] D. Janezic and B. R. Brooks, J. Comput. Chem. **16**, 1543 (1995).
[7] D. Janezic, R. M. Venable, and B. R. Brooks, J. Comput. Chem. **16**, 1554 (1995).
[8] N. Go, T. Noguti, and T. Nishikawa, Proc. Natl. Acad. Sci. U.S.A. **80**, 3696 (1983).
[9] V. Tozzini, Curr. Opin. Struct. Biol. **15**, 144 (2005).
[10] A. R. Atilgan, S. R. Durell, R. L. Jernigan, M. C. Demirel, O. Keskin, and I. Bahar, Biophys. J. **80**, 505 (2001).
[11] K. Hinsen, Proteins **33**, 417 (1998).
[12] F. Tama and Y. H. Sanejouand, Protein Eng. **14**, 1 (2001).
[13] M. M. Tirion, Phys. Rev. Lett. **77**, 1905 (1996).
[14] W. G. Krebs, V. Alexandrov, C. A. Wilson, N. Echols, H. Yu, and M. Gerstein, Proteins **48**, 682 (2002).
[15] I. Bahar and A. J. Rader, Curr. Opin. Struct. Biol. **15**, 586 (2005).
[16] J. Ma, Structure (London) **13**, 373 (2005).
[17] F. Tama and C. L. Brooks, Annu. Rev. Biophys. Biomol. Struct. **35**, 115 (2006).
[18] F. Tama, M. Valle, J. Frank, and C. L. Brooks III, Proc. Natl. Acad. Sci. U.S.A. **100**, 9319 (2003).
[19] Y. Wang, A. J. Rader, I. Bahar, and R. L. Jernigan, J. Struct. Biol. **147**, 302 (2004).
[20] O. Keskin, I. Bahar, D. Flatow, D. G. Covell, and R. L. Jernigan, Biochemistry **41**, 491 (2002).
[21] W. Zheng, B. R. Brooks, and D. Thirumalai, Biophys. J. **93**, 2289 (2007).
[22] F. Tama and C. L. Brooks III, J. Mol. Biol. **345**, 299 (2005).
[23] A. J. Rader, D. H. Vlad, and I. Bahar, Structure (London) **13**, 413 (2005).
[24] F. Tama, F. X. Gadea, O. Marques, and Y. H. Sanejouand, Proteins **41**, 1 (2000).
[25] G. Li and Q. Cui, Biophys. J. **83**, 2457 (2002).
[26] A. D. Schuyler and G. S. Chirikjian, J. Mol. Graphics Modell. **24**, 46 (2005).
[27] W. Zheng and B. R. Brooks, Biophys. J. **89**, 167 (2005).
[28] W. Zheng, J. C. Liao, B. R. Brooks, and S. Doniach, Proteins **67**, 886 (2007).
[29] H. L. Woodcock, W. Zheng, A. Ghysels, Y. Shao, J. Kong, and B. R. Brooks, J. Chem. Phys. **129**, 214109 (2008).
[30] Y. Chen, T. A. Davis, W. W. Hagner, and S. Rajamanickam, ACM Trans. Math. Softw. **35**, 22 (2008).
[31] A. Fiser and A. Sali, Bioinformatics **19**, 2500 (2003).
[32] H. Yu, L. Ma, Y. Yang, and Q. Cui, PLOS Comput. Biol. **3**, e21 (2007).
[33] B. R. Brooks, R. E. Bruccoleri, B. D. Olafson, D. J. States, S. Swaminathan, and M. Karplus, J. Comput. Chem. **4**, 187 (1983).
[34] W. Zheng and B. Brooks, J. Mol. Biol. **346**, 745 (2005).
[35] W. Zheng, B. R. Brooks, and G. Hummer, Proteins **69**, 43 (2007).